Article ID: 1003－6326(2004)01－0156－05

Crystallization behavior of $Ti_{61.67}Zr_{17.15}Ni_{14.80}Cu_{6.38}$ glass-forming alloy①

FAN Jin-duo(范金铎)[1], GAO Yi-qun(高逸群)[2], LI Shi-zeng(黎仕增)[3]
(1. Beijing General Research Institute for Non-ferrous Metals, Beijing 100088, China;
2. Institute of Precious Metals, Kunming 650221, China;
3. Guangxi Institute of Mechanical & Electrical Technology, Nanning 530007, China)

Abstract: $Ti_{61.67}Zr_{17.15}Ni_{14.80}Cu_{6.38}$(atom fraction, %) metallic glass has applications in brazing. Using the hammer-and-anvil technique, $Ti_{61.67}Zr_{17.15}Ni_{14.80}Cu_{6.38}$ metallic glass was prepared. The crystallization behavior for this metallic glass was investigated by differential scanning calorimetry(DSC), X-ray diffractometry(XRD) and transmission electron microscopy(TEM). There are three stages in DSC curves of crystallization. The reduced glass temperature T_{rg} is 0.42. The kinetic parameters of crystallization were calculated by a set of equations of the maximum crystallization rate. The crystalline phase formed in the MSI(Metastable stage I) is Zr_2Cu, in the MSII is α-Ti and in the MSIII is Ti_2Ni. This kind of alloy has lower glass forming ability, and the $Ti_{61.67}Zr_{17.15}Ni_{14.80}Cu_{6.38}$ metallic glass has lower thermal stability.

Key words: $Ti_{61.67}Zr_{17.15}Ni_{14.80}Cu_{6.38}$ metallic glass; crystallization behavior; glass forming ability; brazing
CLC number: TG 139.8; TG 146 **Document code:** A

1 INTRODUCTION

Many conventional brazing alloys containing Ti and Zr are brittle and prohibitively difficult to fabricate into thin shapes conducive to brazing. A conventional form of brazing alloys is paste or plastic bonded tape, in which a powdered form of the alloys is carried by an organic binder. The drawback, however, lies in the residue and porosity. In contract, amorphous filler metals have many advantages, such as ductility, thin gauge, homogeneity of microstructure, low melting temperature, narrow temperature interval of melting and solidification points, short brazing time, high atom diffusion activity and the possibility of having self-fluxing. Amorphous filler metals can result in the production of the same filler-metal composition, but in ductile ribbon form. In addition, ductile foil can be stamped into performs, allowing the gap between the base metal pieces to be more completely and efficiently filled during joining. Applications in which amorphous filler metals are used are varied[1-4].

In previous work, FAN et al[5] studied the brazability of $Ti_{61.67}Zr_{17.15}Ni_{14.80}Cu_{6.38}$ amorphous filler metal. According to the results of shear test, the shear strengths of joints brazed with amorphous filler foils are bigger than those brazed with crystalline filler powders under the same conditions. The size of the central region and the distribution of the common grains formed by mutual crystallization between the filler metal and the base metal are the main factors for the shear strengths of brazed joints.

In this work, $Ti_{61.67}Zr_{17.15}Ni_{14.80}Cu_{6.38}$ metallic glass foils were prepared using the hammer-and-anvil technique in an arc furnace, and investigated its glass forming ability (GFA), the thermal stability and the crystallization behavior were investigated by DSC, DTA, XRD and TEM.

2 EXPERIMENTAL

Ti, Zr, Ni and Cu with purity higher than 99.9% (mass fraction) were used to prepare $Ti_{61.67}Zr_{17.15}Ni_{14.80}Cu_{6.38}$ alloy buttons in an arc furnace. The buttons were broken into small particles, and its mass is 20－40 mg. The particles were then melted and squeezed into foils 40 to 50 μm in thickness one by one using the hammer-and-anvil technique[6, 7]. The cooling rate of this technique is about 1.0×10^6 K/s. A D/MAX-RC type of XRD and a JEM-2000EX type transmission electron microscope were used to examine whether the rapidly quenched foils were amorphous or not and to determine their constitutions and microstructures. A THERMOFLEX differential scanning calorimeter was used to obtain thermographs at various rates: 2.5, 5, 10 and 20 K/min. 16 to 24 mg samples were heated in a Pt pan surrounded by a stream of purified argon gas at 50 cm^3/min to 55 cm^3/min during analysis. Prior to filling with purified argon gas, the DSC system was evacuated to 6.7 Pa. Argon gas was purified through

① **Foundation item:** Project(ZSK91-D0079) supported by the Non-Ferrous Metals Industry Association of China
Received date: 2003－03－19; **Accepted date:** 2003－06－10
Correspondence: FAN Jin-duo, Senior engineer, Master; Tel: +86-10-80105153; Fax: +86-10-62051917; E-mail: jinduo@yeah.net

4A molecular sieve under 90 K. The temperature was calibrated using the melting endotherms of pure In, Sn, Pb and Al.

The melting temperatures of $Ti_{61.67}Zr_{17.15}Ni_{14.80}Cu_{6.38}$ alloy were measured using a THERMOFLEX high temperature differential thermal analysis (DTA).

Using DSC, XRD and TEM, the behavior of crystallization for $Ti_{61.67}Zr_{17.15}Ni_{14.80}Cu_{6.38}$ metallic glass was investigated. $Ti_{61.67}Zr_{17.15}Ni_{14.80}Cu_{6.38}$ metallic glass was annealed for 2 h at 993 K. Before annealing, the system was evacuated to 6.7×10^{-3} Pa and then filled argon gas to 1.5×10^{4} Pa shown in the regulator. Using a twin-jet electropolisher with a solution of 95% CH_3COOH + 5% $HClO_4$, the samples were prepared into thin films.

3 RESULTS

The as-prepared samples were amorphous. The X-ray diffraction patterns of $Ti_{61.67}Zr_{17.15}Ni_{14.80}Cu_{6.38}$ foils only contain an extremely broadened line followed by a smaller broadened line. The electron diffraction patterns of the foils only contain diffuse halos typical for amorphous phase. No signs of crystalline phases were found in the transmission electron micrographs.

The exothermic curve for $Ti_{61.67}Zr_{17.15}Ni_{14.80}Cu_{6.38}$ metallic glass at a heating rate of 10 K/min is shown in Fig. 1. There are three exothermic stages: MS I, MS II and MS III in the DSC curves of crystallization. From the DSC curves, parameters, such as the glass transition temperature (T_g), the peak temperature (T_p) and the maximum rate of crystallization $(dx/dt)_p$ for each stage at various heating rates B= 2.5, 5, 10 and 20 K/min, can be obtained. For the MS I and MS II, the heights of the crystallization peaks were too small to be determined at each heating rate. The enthalpy of crystallization ΔH for each exothermic stage was calculated from the area under the peaks. The results are listed in Table 1. n is the Avrami exponent; E is the activation energy of crystallization; k_p is the rate constant at T_p.

Fig. 2 shows a high temperature DTA scan of $Ti_{61.67}Zr_{17.15}Ni_{14.80}Cu_{6.38}$ metallic glass heated at 10 K/min. The alloy begins to melt at the solidus temperature T_{sol}= 1 133 K followed by complete melting at the liquidus temperature T_{liq} = 1 252 K. The reduced glass transition temperature T_{rg}(T_{rg}= T_g/ T_{liq}) of this alloy is 0.42.

In order to investigate the structures in each stage of crystallization, the $Ti_{61.67}Zr_{17.15}Ni_{14.80}Cu_{6.38}$

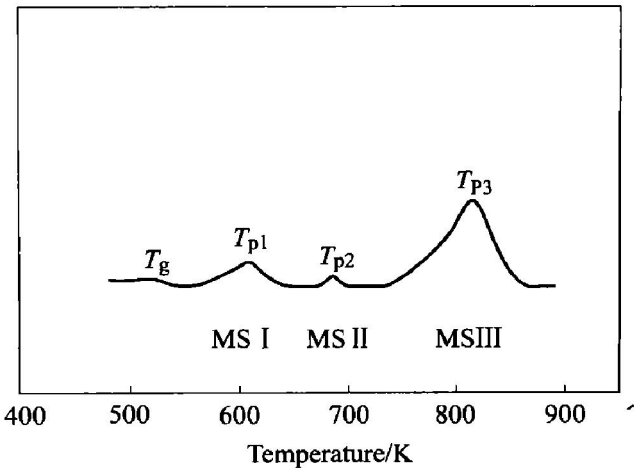

Fig. 1 DSC scan of $Ti_{61.67}Zr_{17.15}Ni_{14.80}Cu_{6.38}$ metallic glass

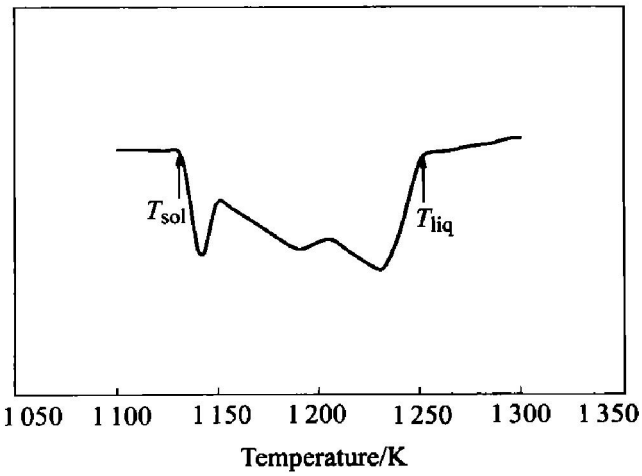

Fig. 2 High temperature DTA scan of $Ti_{61.67}Zr_{17.15}Ni_{14.80}Cu_{6.38}$ metallic glass

Table 1 Kinetic parameters of crystallization in $Ti_{61.67}Zr_{17.15}Ni_{14.80}Cu_{6.38}$ metallic glass

Stage	B/ (K·min^{-1})	T_p(or T_g)/ K	$(dx/dt)_p$/ $10^{-2}s^{-1}$	E/ (kJ·mol^{-1})	k_p/ $10^{-2}s^{-1}$	n	ΔH/ (J·g^{-1})
MSG	2.5	503					
	5	519					
	10	530					
	20	546					
MS I	2.5	576					
	5	591		131			7.78
	10	608					
	20	623					
MS II	2.5	656					
	5	669		186			2.59
	10	685					
	20	698					
MS III	2.5	793	0.234 8	309	0.245 6	2.6	15.06
	5	803	0.380 8		0.479 5	2.2	
	10	815	0.873 4		0.929 1	2.5	
	20	827	1.372 3		1.815 7	2.0	

metallic glass was heated at a heating rate of 10 K/min to various temperatures (610, 693, 823 and 993 K) in flowing purified argon gas in DSC. As shown in Fig. 1, 610, 693 and 823 K are between the top and the end temperatures of the stages of MS Ⅰ, MS Ⅱ and MS Ⅲ, respectively. At a heating rate of 10 K/min, 993 K is in the completely crystallized region. The X-ray diffraction patterns (Cu K_α) are shown in Fig. 3 for samples heated to 610, 693, 823 and 993 K, respectively. When the values of interplanar distances d and the relative intensities I/I_0 are compared with the standard values listed in the Inorganic Index to the Powder Diffraction File[8], the crystalline phases in each sample can also be determined, as shown in Table 2.

As shown in Fig. 3, the diffraction peaks become sharper with increasing temperatures, the main diffraction peaks which occur at the interplanar distance between 2.42 Å and 2.17 Å are those of Zr_2Cu, Ti_2Ni and α-Ti crystalline phases. It is concluded that the crystalline phase formed in the MSI is Zr_2Cu, that in the MSII is α-Ti, and that in the MSIII is Ti_2Ni.

The transmission electron micrograph of the complete crystallization samples are obtained and shown in Fig. 4. From the transmission electron micrograph and the electron diffraction patterns, it is found that the phase, which contains thin branches, is Ti_2Ni, and the other is Zr_2Cu. Being easily etched, α-Ti can not be found.

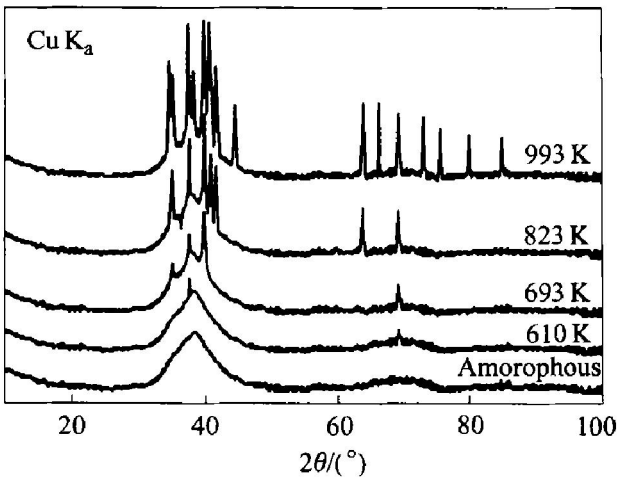

Fig. 3 XRD of $Ti_{61.67}Zr_{17.15}Ni_{14.80}Cu_{6.38}$ metallic glass

4 DISCUSSION

The glass forming compositions in many alloy systems containing Ti and Zr have been investigated, such as Ti-Zr-Ni and Ti-Zr-Ni-Cu alloy system by Molokanov et al[9, 10], Ti-Zr-Cu by Massalsaki et al[11], Ti-Zr-Ni-Cu by Lin et al[12] and Rabinkin et

Table 2 Interplanar distances relative intensities I/I_0 of X-ray diffraction peaks and associated phases in $Ti_{61.67}Zr_{17.15}Ni_{14.80}Cu_{6.38}$ metallic glass

Peak	610 K		693 K		823 K		993 K	
	d	I/I_0	d	I/I_0	d	I/I_0	d	I/I_0
1	2.392	100	2.571	55	2.565	64	2.591	76
2	1.358	42	2.394	80	2.396	85	2.567	68
3			2.261	100	2.253	100	2.398	98
4			1.356	37	2.212	75	2.361	70
5					2.165	67	2.259	100
6					1.479	40	2.216	99
7					1.359	38	2.171	73
8							2.04	51
9							1,457	45
10							1,411	45
11							1.357	46
12							1.295	44
13							1.275	37
14							1.197	33
15							1.14	32
Phases	Zr_2Cu		Zr_2Cu α-Ti		Zr_2Cu α-Ti Ti_2Ni		Zr_2Cu α-Ti Ti_2Ni	

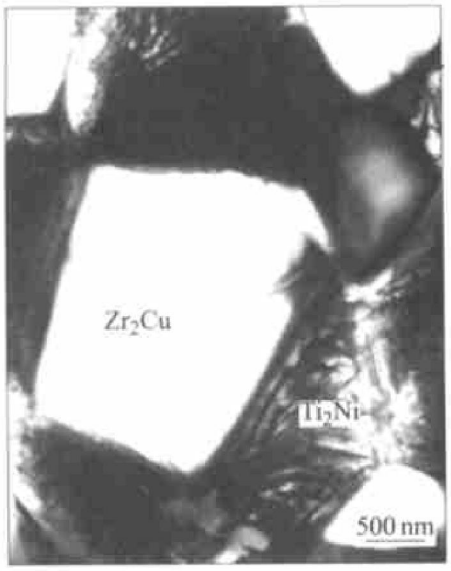

Fig. 4 Micrograph of $Ti_{61.67}Zr_{17.15}Ni_{14.80}Cu_{6.38}$ metallic glass annealed for 2 h at 993 K

al[2]. Many of these glass-forming compositions have good glass forming ability (GFA). The reduced glass transition temperature T_{rg} of the glass forming alloys plays an important role in determining the GFA of alloys. Alloys having higher T_{rg} generally exhibit better GFA[13]. T_{rg} of $Ti_{34}Zr_{11}Cu_{47}Ni_8$ alloy is 0.57, and the critical cooling rate for the glass formation is about 250 K/s or lower[12]. T_{rg} of $Zr_{41.2}Ti_{13.8}Cu_{12.5}Ni_{10}Be_{22.5}$ alloy is 0.67, and the critical cooling rate for the glass formation is 1 K/s[14].

T_{rg} of $Ti_{61.67}Zr_{17.15}Ni_{14.80}Cu_{6.38}$ alloy is 0.42, and this suggests that the GFA of this glass-forming alloy is inferior.

GAO et al[15, 16] have proposed a set of equations for the maximum rate of crystallization to obtain the kinetic parameters of crystallization from the results of DSC. When the crystallization behavior obeys the Johnson-Mehl-Avrami transformation model, they are as follows:

$$x = 1 - \exp[-(kt)^n] \quad (1)$$

$$d[\ln(dx/dt)_p]/d(T_p^{-1}) = -E/R \quad (2)$$

$$k_p = BE/(RT_p^2) = k_0\exp[-E/(RT_p)] \quad (3)$$

$$(dx/dt)_p = 0.37nk_p \quad (4)$$

where x is the volume fraction crystallized; k is the rate constant; t is the time of crystallization; n is the Avrami exponent; $(dx/dt)_p$ is the maximum rate of crystallization at peak temperature T_p; E is the activation energy of crystallization; R is the gas constant; k_p is the rate constant at T_p; B is the heating rate; k_0 is the frequency factor.

If the plot of $(dx/dt)_p$ against T_p^{-1} shows no linearity, the activation energy of crystallization cannot be obtained from Eqn. (2). In that case, the Kissinger equation or its simplified form can also be used for calculating the activation energy of crystallization[15, 16]:

$$-E/R = d(\ln B)/d(T_p^{-1}) \quad (5)$$

The plot of $\log(dx/dt)_p$ against T_p^{-1} for the MSIII is shown in Fig. 5. Since this shows a straight line, Eqns. (2)-(4) can be used to calculate the kinetic parameters of crystallization from the slope. The resulting values of the activation energy E, the rate constant k_p and the Avrami exponent n are listed in Table 1.

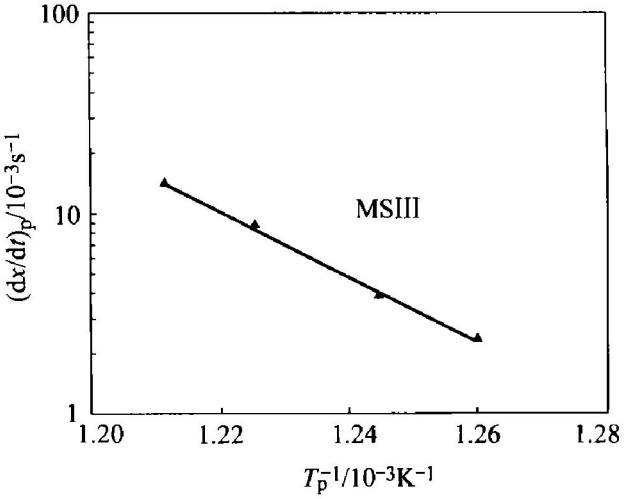

Fig. 5 Plot of $\lg(dx/dt)_p$ against T_p^{-1} for MS III of $Ti_{61.67}Zr_{17.15}Ni_{14.80}Cu_{6.38}$ metallic glass

$\log B$ against T_p^{-1} for MS I and MS II is listed in Fig. 6. From the slopes of the straight lines in Fig. 6 and Eqn. (5), the values of the activation energies of crystallization E for the MS I and MS II of this metallic glass can be obtained and they are listed in Table 1, too.

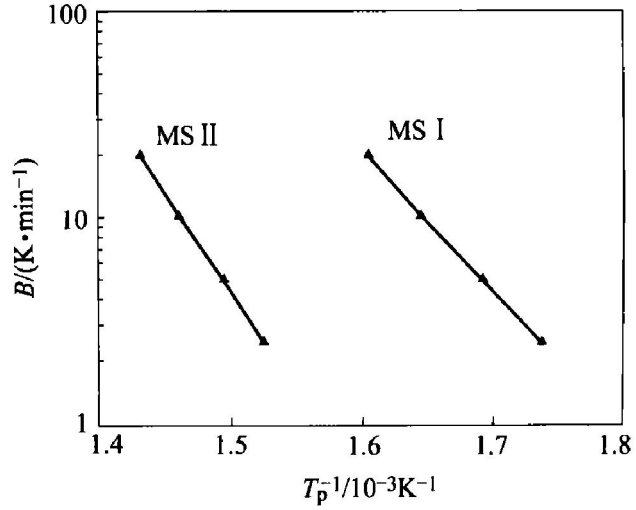

ig. 6 Plots of $\lg B$ against T_p^{-1} for MS I and MS II of $Ti_{61.67}Zr_{17.15}Ni_{14.80}Cu_{6.38}$ metallic glass

Comparing with $Ti_{45.50}Zr_{23.80}Ni_{15.91}Cu_{14.70}$ and $Ti_{50}Ni_{10}Cu_{40}$ metallic glasses[17, 18], the values of activation energy of crystallization for $Ti_{61.67}Zr_{17.15}Ni_{14.80}Cu_{6.38}$ metallic glass are smaller. In general, the smaller the activation energy of crys-

tallization, the lower the thermal stability of the metallic glass. The thermal stability of $Ti_{61.67}Zr_{17.15}Ni_{14.80}Cu_{6.38}$ metallic glass is lower.

According to the theory of Christian[19], the Avrami exponent n and the nucleation rate in crystallization are related: if n is 3, the nucleation rate is zero; if n is 2, the grain edge nucleation occurs after saturation. In MS III, the values of n change from 2.0 at B= 20 K/min to 2.6 at B= 2.5 K/min. This suggests that the nucleation rate at B= 2.5 and 10 K/min is about zero, and that at 5 and 20 K/min the grain edge nucleation occurs after saturation.

The atomic volume ratio of Zr/Cu (1.95) is the biggest in Ti-Zr-Ni-Cu system[20]. With the content of Zr and Cu decreasing, the crystallization behavior of the metallic glasses in Ti-Zr-Ni-Cu system has been changed distinctly. There are two exothermic stages in the DSC curves of $Ti_{45.50}Zr_{23.89}Ni_{15.91}Cu_{14.70}$ metallic glass. The crystalline phases Ti_2Ni, Zr_2Cu and α-Ti were formed in MS I at the same time, and a recrystallization process occurs in MS II[17]. There are three stages, therefore, in the DSC curves of $Ti_{61.67}Zr_{17.15}Ni_{14.80}Cu_{6.38}$ metallic glass, the crystalline phase formed in the MSI is Zr_2Cu, that in the MSII is α-Ti and that in the MSIII is Ti_2Ni.

5 CONCLUSIONS

1) Using the hammer-and-anvil technique, $Ti_{61.67}Zr_{17.15}Ni_{14.80}Cu_{6.38}$ metallic glass was prepared. This metallic glass has applications for brazing.

2) There are three exothermic stages of crystallization in the DSC curves for $Ti_{61.67}Zr_{17.15}Ni_{14.80}Cu_{6.38}$ metallic glass.

3) For $Ti_{61.67}Zr_{17.15}Ni_{14.80}Cu_{6.38}$ metallic glass, the Avrami exponent in MSIII lies between 2.0 and 2.6.

4) The reduced glass transition temperature T_{rg} of $Ti_{61.67}Zr_{17.15}Ni_{14.80}Cu_{6.38}$ metallic glass is 0.42, and this alloy has lower glass-forming ability.

5) The phases Zr_2Cu, α-Ti and Ti_2Ni were formed in MS I, MS II and MS III of crystallization for $Ti_{61.67}Zr_{17.15}Ni_{14.80}Cu_{6.38}$ metallic glass, respectively.

6) $Ti_{61.67}Zr_{17.15}Ni_{14.80}Cu_{6.38}$ metallic glass has lower thermal stability.

REFERENCES

[1] Decristofaro N, Henschel C. Brazing foil[J]. Weld J, 1978, 57(7): 33-38.

[2] Rabinkin A, Liebermann H, Pounds S, et al. Amorphous Ti-Zr- base metglas brazing filler metals[J]. Scr Metall Mater, 1991, 25(2): 399-404.

[3] Kalin B A, Fedotov V T, Sevryukov O N, et al. Application of amorphous and microcrystalline filler metals for brazing of beryllium with metals[J]. J Nucl Mater, 1996, 233-237: 945-948.

[4] Kalin B A, Fedotov V T, Grigoriev A E, et al. Application of amorphous filler metals in production of fusion reactor high heat flux components[J]. Fus Eng Des, 1995, 28(16): 119-124.

[5] FAN Jin-duo, GAO Yi-qun, YANG Jia-ming, et al. Study on amorphous $Ti_{61.67}Zr_{17.15}Ni_{14.80}Cu_{6.38}$ brazing filler metals [A]. Proc of Internat Conf on Engineering and Technological Sciences 2000- Advanced Materials, Vol. 1[C]. Beijing: New World Press, 2000. 287-290.

[6] CUI Ru-jian, GAO Yi-qun, MAO Yong. An instrument for rapid quenching[P]. CN87215425U, 1988-06-29.

[7] Ohring M, Haldipur A. A versatile arc melting apparatus for quenching molten metals and ceramics[J]. Rev Sci Instrum, 1971, 42: 530-531.

[8] Leonard G B. Inorganic Index to the Powder Diffraction File, Joint Committee on Powder Diffraction Standards [M]. PA: Swarthmore, 1972.

[9] Molokanov V V, Chebotnikov V N. Quasicrystals and amorphous alloys in Ti-Zr-Ni system: glass forming ability, structure and properties[J]. J Non-Cryst Solids, 1990, 117-118: 789-792.

[10] Molokanov V V, Chebotnikov V N. Glass forming ability, structure and properties of Ti and Zr- intermetallic compound based alloys[J]. Key Eng Mater, 1990, 40-41: 319-332.

[11] Massalsaki T B, Woychik C G, Dutkiewicz J. Solidification structures in rapidly quenched Cu-Ti-Zr alloys [J]. Metall Trans A, 1988, 19A: 1853-1860.

[12] Lin X H, Johnson W L. Formation of Ti-Zr-Cu-Ni bulk metallic glasses[J]. J Appl Phys, 1995, 78(11): 6514-6519.

[13] Spaepen F, Turnbul l D. Formation of metallic glasses [A]. Proceedings of the Second International Conference on Rapidly Quenched Metals[C]. Cambridge, MA: MIJ Press, 1976. 205-229.

[14] Kim Y J. Busch R, Johnson et al. Metallic glass formation in highly undercooled $Zr_{41.2}Ti_{13.8}Cu_{12.5}Ni_{10.0}Be_{22}$ during containerless electrostatic levitation processing [J]. Appl Phys Lett, 1994, 65: 2136-2140.

[15] GAO Yi-qun, WANG We-go. On the activation energy of crystallization in metallic glasses[J]. J Non-Cryst Solids, 1986, 81: 129-134.

[16] GAO Yi-qun, WANG We-go, ZHENG Fu-qian, et al. On the crystallization kinetics of $Pd_{80}B_4Si_{16}$ glass[J]. J Non-Cryst Solids, 1986, 81: 135-139.

[17] FAN Jin-duo, GAO Yi-qun, HU Chang-yi, et al. Crystallization behavior of $Ti_{45.50}Zr_{23.89}Ni_{15.91}Cu_{14.70}$ metallic glass[J]. Mat Sci Eng A, 2001, 304-306: 367-370.

[18] Murty B S, Rao M M, Ranganathan S. Differences in the glass-forming ability of rapidly solidified and mechanically alloyed Ti-Ni-Cu alloys[J]. Mat Sci Eng A, 1995, 196: 237-241.

[19] Christian J W. The Theory of Transformation in Metals and Alloys. 2nd ed[M]. Oxford: Pergamon Press, 1975.

[20] Amiya K, Nishiyama N, Inoue A, et al. Mechanical strength and thermal stability of Ti-based amorphous alloys with large glass-forming ability[J]. Mat Sci Eng A, 1994, 179-180: 692-69.

(Edited by LI Xiang-qun)